Tetragonal structure of $CaSiO_3$ perovskite above 20 GPa

Sang-Heon Shim,[1] Raymond Jeanloz,[1] and Thomas S. Duffy[2]

Received 21 August 2002; revised 14 October 2002; accepted 18 October 2002; published 19 December 2002.

[1] High-resolution synchrotron X-ray diffraction measurements were performed at 20–46 GPa on $CaSiO_3$ perovskite (Ca-pv) synthesized in a laser heated diamond cell. After heating, we observed peak splittings for the cubic 200 and 211 diffraction lines, attributable to a tetragonal distortion of Ca-pv. The bulk modulus of the tetragonal phase is 255 ± 5 GPa for $K_{0T}' = 4$. The observed intensities and d-spacings of the split lines indicate that the *c*-axis is shorter than the *a*-axes ($c/a = 0.993 - 0.996$). This is compatible with either SiO_6 octahedron rotation around the *a*-axes or SiO_6 octahedron distortion (shorter Si-O bonds along the *c*-axis than the *a*-axes), provided that the observed phase has a tetragonal unit cell. These structural distortions in Ca-pv can affect its physical properties and capacity for large cations. *INDEX TERMS:* 3620 Mineralogy and Petrology: Crystal chemistry; 3924 Mineral Physics: High-pressure behavior; 3954 Mineral Physics: X ray, neutron, and electron spectroscopy and diffraction; 8124 Tectonophysics: Earth's interior—composition and state (old 8105). **Citation:** Shim, S.-H., R. Jeanloz, and T. S. Duffy, Tetragonal structure of $CaSiO_3$ perovskite above 20 GPa, *Geophys. Res. Lett.*, *29*(24), 2166, doi:10.1029/2002GL016148, 2002.

1. Introduction

[2] $CaSiO_3$ perovskite (Ca-pv) is believed to be an important phase in the Earth's transition zone and lower mantle. Experimental studies have shown that Ca-pv forms in mantle-relevant compositions under deep Earth conditions [*Funamori et al.*, 2000; *Wood*, 2000], and its physical properties are important to understanding the transition zone seismic structure [*Sinogeikin and Bass*, 2002].

[3] The stability and equation of state of Ca-pv have been investigated to core-mantle boundary (CMB) conditions [*Mao et al.*, 1989; *Shim et al.*, 2000b] by energy-dispersive synchrotron X-ray diffraction (XRD) in the laser-heated diamond anvil cell (DAC). Within the resolution of these studies, $CaSiO_3$ has a cubic perovskite structure ($Pm\bar{3}m$). However, a theoretical study [*Stixrude et al.*, 1996] has proposed that the tetragonal phase of Ca-pv is more stable at all pressures at 0 K, and a tetragonal-to-cubic transition may occur at lower mantle conditions. An even lower symmetry (orthorhombic) has been recently proposed by other studies [*Akber-Knutson et al.*, 2002; *Magyari-Köpe et al.*, 2002] [for a detailed review of studies of Ca-pv, see *Shim et al.*, 2000b]. In order to investigate possible structural distortions in Ca-pv, we performed high-resolution angle-dispersive diffraction measurements.

2. Experimental Technique

[4] Pure natural wollastonite powder was mixed with platinum which serves as both a pressure standard [*Holmes et al.*, 1989] and laser absorber. The sample was loaded into a DAC together with argon as both a pressure medium and thermal insulator. We also loaded ruby chips at the edge of samples as a secondary pressure calibrant. In order to synthesize Ca-pv and/or anneal differential stresses, samples were heated for at least 15 minutes to more than 1500 K before each XRD measurement by scanning a continuous Nd:YAG laser across the sample.

[5] We conducted high-resolution diffraction measurements at the B-2 sector of the Cornell High Energy Synchrotron Source and the 10-2 sector of the Stanford Synchrotron Radiation Laboratory. Image plates (IPs) (2048 × 2048 and 4096 × 8192 pixels) were used at 20–27 cm distances from the samples to collect diffraction by monochromatic X-rays (24.999 and 17.038 keV). Two-dimensional diffraction images were integrated to one-dimensional patterns after correcting for IP tilt using the SImPA program [*Desgreniers*, 1998]. Sample-to-IP distance and IP tilting were measured for each data acquisition by collecting XRD patterns of MgO or NaCl loaded on the table face of the diamond anvil. Two different types of DACs were used: symmetric cells whose conical aperture allows integration over a 140° range of the diffraction rings for d-spacings larger than 1.5 Å, and Mao-Bell cells whose slot-type aperture allows to cover a wider range of d-spacing (>1.3 Å) for a 7–15° portion of the rings.

[6] Non-linear regressions were performed for the measured d-spacings to obtain unit-cell parameters using the Unitcell program [*Holland and Redfern*, 1997]. Rietveld refinements were also performed for the measured patterns using GSAS [*Larson and Von Dreele*, 1988]. We refined unit-cell parameters, atomic positions, and thermal factors of atoms with preferred orientation correction.

3. Results and Discussions

[7] A total of six diffraction images was collected at pressures of 19.7, 24.2, 25.2, 26.6, 36.1, and 45.8 GPa for four different samples. Peak splittings were observed for the 200_C and 211_C diffraction rings (the subscript "C" indicates the index for a cubic unit cell with the $Pm\bar{3}m$ space group) for all of the images measured above 20 GPa (Figure 1). In the images (e.g., Figure 1a), the 200_C diffraction ring is much broader and spottier than other Ca-pv diffraction rings. The dots in the ring are clearly split and lie along two separate rings. The splittings are also detected in the integrated one-dimensional diffraction patterns (Figure 1b and 1c). The splittings are not clear for the sample below 20 GPa. However, the peak width of the 200_C line is almost a

[1]Department of Earth and Planetary Science, University of California, Berkeley, California, USA.
[2]Department of Geosciences, Princeton University, Princeton, New Jersey, USA.

0094-8276/02/2002GL016148$05.00

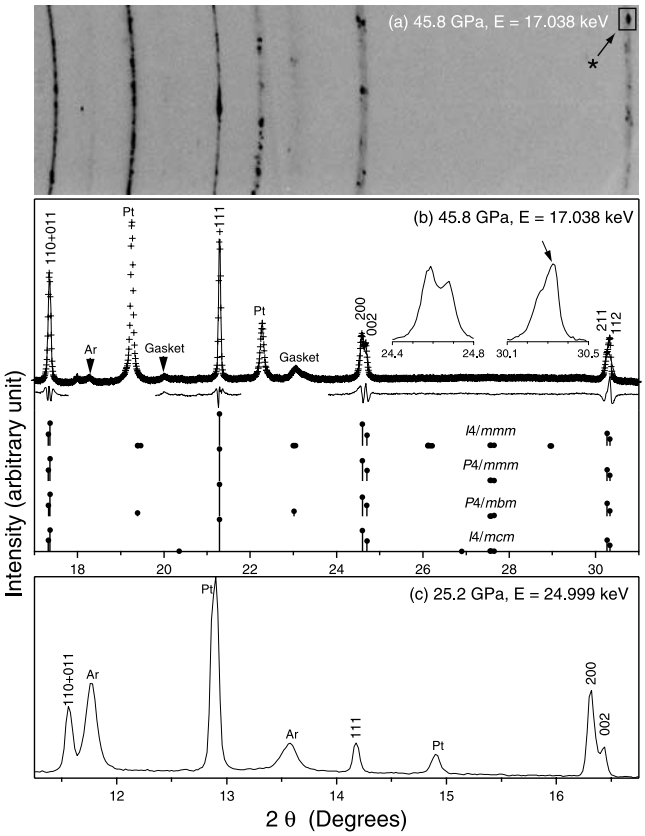

Figure 1. XRD patterns of Ca-pv at high pressure. (a) Portion of a diffraction image at 45.8 GPa. (b) Integrated one dimensional pattern of (a) (crosses). A Rietveld refinement result based on the *P*4/*mmm* space group is shown as a solid line overlapping the crosses. The solid line in the mid-portion shows the difference between observed and calculated patterns. Calculated diffraction patterns for *I*4/*mmm*, *P*4/*mmm*, *P*4/*mbm*, and *I*4/*mcm* space groups (vertical bars below) are shown for comparison. The insets show the peak splittings of 200_C and 211_C diffraction lines of Ca-pv. Diffraction lines in (a) and (b) are roughly aligned for comparison (*x*-axis in (a) is a length scale based on IP dimension, not an angle scale). (c) Integrated XRD pattern of Ca-pv measured at 25.2 GPa. This pattern was obtained by integrating a larger portion of the rings (140°). Indexed lines are the diffraction lines of Ca-pv based on *P*4/*mmm* (Pt: platinum, Ar: argon).

factor of 1.5 greater than those of other diffraction lines at these pressures [*Wang and Yagi*, 1998], indicating a possible tetragonal distortion below 20 GPa.

[8] Peak splittings were detected more readily after laser heating. Even after annealing, some samples show less clear peak splittings, possibly because these samples contain less pressure medium (argon) as shown by the weaker diffraction from argon in Figure 1b relative to 1c.

[9] The observed peak splittings are consistent with those expected for a tetragonal distortion: larger splittings will be observed for the diffraction lines from the planes perpendicular to the cubic unit-cell axes, i.e., peak splittings will be largest in the order of 200_C, 211_C, and 110_C. We observed the most pronounced splitting for the 200_C diffraction line (Figure 1). Both individual peak fitting and Rietveld refinement yield identical results for the unit-cell parameters of Ca-pv (Figure 2). In addition, the refined values of the unit-cell parameters are insensitive to the space group used in Rietveld refinements. All data obtained show 0.4% shorter *c*-axis than *a*-axes, except for a single data point, and this ratio (*c*/*a*) does not change with compression (Figure 2b). This amount of distortion is smaller than the estimated resolution of energy-dispersive XRD [*Shim et al.*, 2000a].

[10] The volume of Ca-pv from the present study lies between the compression curves of *Mao et al.* [1989] and *Shim et al.* [2000a] (Figure 2a). Fitting our data points to the Birch-Murnaghan equation assuming that the pressure derivative of the isothermal bulk modulus is 4 and the volume at ambient conditions is 45.58 $Å^3$ [*Wang et al.*, 1996], the isothermal bulk modulus of Ca-pv is 255 ± 5 GPa, which is lower than the values of earlier measurements (281–325 GPa) [*Tamai and Yagi*, 1989; *Mao et al.*, 1989; *Yagi et al.*, 1989; *Tarrida and Richet*, 1989] but higher than more recent values (232–236 GPa) [*Wang et al.*, 1996; *Shim et al.*, 2000a]. However, it should be noted that all previous measurements were analyzed based on a cubic unit cell.

[11] Insights into the distortion in Ca-pv can be obtained from the intensities of split lines of 200_C. We always observed this line splits such that the more intense peak of the doublet occurs at lower angle (Figure 1b and 1c). Since minor structural changes are expected from the observed XRD patterns, we can assume that the tetragonal structure will be close to the cubic perovskite structure. Under this assumption, the more intense peak of the 200_C doublet corresponds to a more repetitive feature of the crystal structure. This implies that the intense line should originate from atomic planes normal to the two identical *a*-axes of the tetragonal unit cell and the less intense line should originate from the planes normal to the *c*-axis. Thus, we assign 200_T (the subscript "T" indicates an assignment

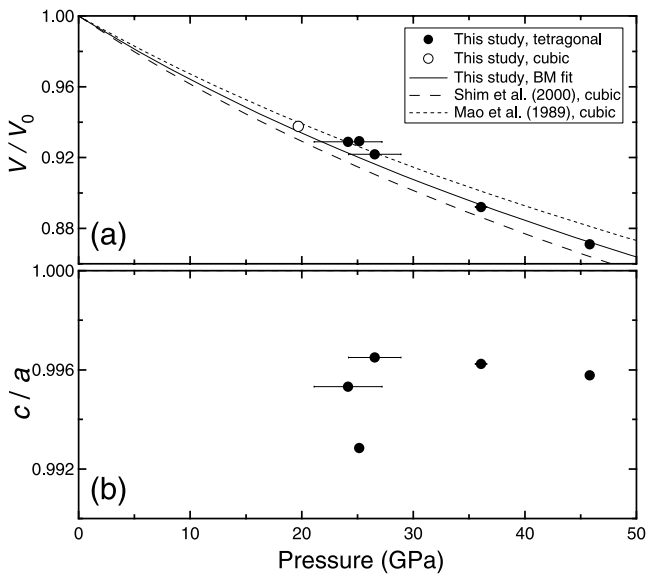

Figure 2. (a) Volume and (b) *c*/*a* ratio of tetragonal Ca-pv. The cell parameters of tetragonal Ca-pv are calculated using the *P*4/*mmm* perovskite structure. At 19.7 GPa, we performed the refinement with a cubic cell (open symbol). Error bars hereafter are 1σ uncertainties.

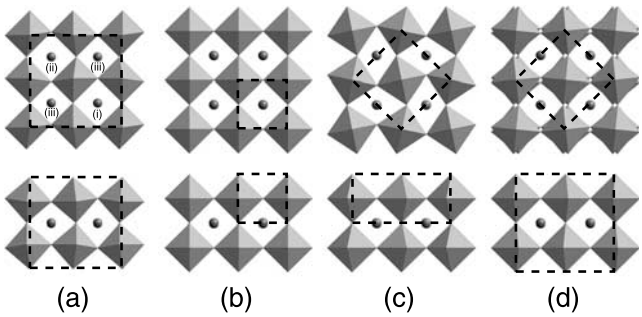

Figure 3. Possible crystal structures of Ca-pv. (a) *I*4/*mmm*, (b) *P*4/*mmm*, (c) *P*4/*mbm*, and (d) *I*4/*mcm*. The octahedra represent SiO_6 and the balls represent Ca atoms. Dashed rectangles show unit cells. Atomic positions were obtained from the Rietveld refinements at 45.8 GPa. Projections along the *c*-axes are shown above and projections along the *a*-axes are shown below.

using a tetragonal cell with the *P*4/*mmm* space group) to the more intense line and 002_T to the less intense line.

[12] Indeed, if we index differently in both unit-cell refinements and Rietveld refinements, i.e., 200_T for the split line at higher angle and 002_T for the split line at lower angle, the refinements diverge. In addition, our interpretation is confirmed by the integration of the large portions of the diffraction rings (Figure 1c), which should be less affected by preferred orientation. According to this assignment, the split line of 211_C at lower angle should be more intense. However, Figure 1b shows a different trend than expected. In other XRD patterns, this line indeed splits with a more intense line at a lower angle. Only a small portion of the rings could be measured for this line due to the limited diamond cell aperture for the high-angle diffraction line. In fact, the excess intensity in 112 is mainly due to the strong diffraction spot indicated by an asterisk in Figure 1a. Thus, this apparent discrepancy is likely due to preferred orientation.

[13] It is known that distortion in many perovskite-structured materials is caused by the rotation of rigid octahedra [*Glazer*, 1972; *Woodward*, 1997]. Octahedron rotation around a particular axis usually decreases the unit-cell dimensions along a plane normal to the rotation axis. As the *c*-axis is shorter than the *a*-axes in Ca-pv, octahedron rotation around the *a*-axes is expected (Figure 3a), if the SiO_6 octahedra are rigid. The space group of this rotation type is *I*4/*mmm*. Rietveld refinements with this space group show that the octahedron rotates by $4.9 \pm 1.7°$ at 45.8 GPa. We also find that the Si-O bond length along the *c*-axis is shorter by $0.6 \pm 0.3\%$ than those along the *a*-axes (Figure 4). An interesting feature of this structure is that it has three crystallographically different Ca sites (Figure 3a).

[14] It is worth mentioning that some degree of preferred orientation may be directly inferred from the measured patterns. For example, intensities are greatest in the order of 111, 110 + 011, and 200 + 002 in Figure 1b, but 200 + 002, 110 + 011, and 111 in Figure 1c. Since Figure 1c is obtained by integrating a much larger portion of the diffraction rings, the excess intensity of 111 diffraction in Figure 1b is due to preferred orientation along this direction. We corrected for preferred orientation using the March-Dollase function [*Dollase*, 1986] for the refinement of Figure 1b.

[15] We also performed Rietveld refinements with a space group allowing only SiO_6 octahedron distortion without rotation (*P*4/*mmm*). This tetragonal perovskite structure has almost the same unit cell as cubic perovskite (Figure 3b), the only difference being that the *c*-axis is no longer identical to the *a*-axes. In this structure, the atomic positions are determined from the unit-cell parameters. This simple model provides a good fit to the observed XRD pattern, with almost identical residuals (R_{wp} = 6.9%) to the *I*4/*mmm* case (R_{wp} = 7.1%). In these two extreme cases (with and without octahedron rotation), the refinements always require the octahedron to be distorted. This implies that the tetragonal distortion of Ca-pv is associated with anisotropy of the octahedra, with or without accompanying octahedra rotation.

[16] We also fit the observed XRD patterns with a model that has octahedron rotation around the *c*-axis, such as *P*4/*mbm* and *I*4/*mcm* (Figure 3c and 3d). Octahedron rotation around the *c*-axis leads to relative contraction of the *a*-axes, whereas our measured XRD patterns show relative contraction of the *c*-axis. Indeed, if these models were used, longer Si-O bond lengths along the *a*-axes (0.6–2.5%) are obtained to counterbalance the *a*-axis contraction from the assumed octahedron rotation around the *c*-axis.

[17] In fact, anisotropic SiO_6 octahedra can also be found in $MgSiO_3$ perovskite (Mg-pv) (Figure 4). Three different pairs of Si-O bonds exist in the *Pbnm* space group of Mg-pv, whereas two different pairs of Si-O bonds exist in the tetragonal perovskite structures. The Si-O bond lengths in Mg-pv measured by single crystal XRD studies [*Horiuchi et al.*, 1987; *Kudoh et al.*, 1987; *Ross and Hazen*, 1989] are roughly grouped into two based on their length: two pairs of Si-O bonds are longer than the other pair of Si-O bonds. In addition, the compressibilities of these two groups of Si-O bonds in Mg-pv are well aligned with those in Ca-pv (Figure 4). This may be an indication of intrinsic anisotropy of the Si-O bond in these silicate perovskites.

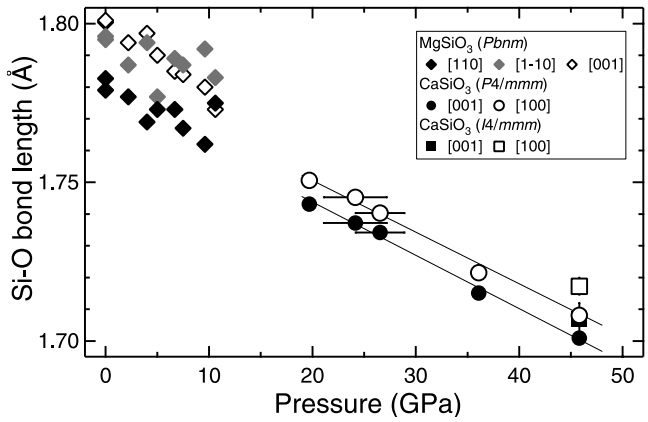

Figure 4. Si-O bond lengths in Ca-pv at high pressures (solid circles and squares: Si-O bond along *c*-axis; open circles and squares: Si-O bond along *a*-axes). Si-O bond lengths were calculated with both *P*4/*mmm* (circles) and *I*4/*mmm* space groups (squares). Solid lines are to guide the eye. We also include the Si-O bond lengths in Mg-pv at high pressures from single crystal XRD studies [*Horiuchi et al.*, 1987; *Kudoh et al.*, 1987; *Ross and Hazen*, 1989] with their closest crystallographic orientations (diamonds).

[18] It is important to characterize the differential stress in our sample to understand the stability of the distorted structure. The differential stress in the sample can be estimated using the relative diffraction peak (111 and 200) shift of platinum and the lattice strain theory [*Singh*, 1993]. Using the ambient pressure value of the elastic anisotropy of platinum, the differential stress is less than 0.2 GPa at 46 GPa. In addition, the fact that the peak splitting is more pronounced with more pressure medium (i.e., much less differential stress) (Figure 1c) indicates that the distortion is not induced by differential stress.

[19] However, it should be noted that *I*4/*mmm* and *P*4/*mmm* space groups are extremely rare among known perovskite structures [e.g., *Woodward*, 1997]. Furthermore, in more recent first-principles calculations [*Akber-Knutson et al.*, 2002; *Magyari-Köpe et al.*, 2002], an orthorhombic structure has been proposed for the structure in the ground state. Based on the observed peak width of diffraction lines, the resolution limit of the technique we used is 0.13%. Thus, if a phase with lower symmetry than tetragonal exists, the distortion should be less than 0.13%. Further studies are necessary to confirm the space group assignment and to investigate the possibility of lower symmetry structures.

[20] Because our diffraction patterns were measured after laser heating, it is not clear whether the tetragonal structure is stable at simultaneously high temperature and pressure. Although the tetragonal structure may be formed at high temperature and preserved during temperature quench, it is also possible that Ca-pv has a higher symmetry, such as a cubic structure, at high temperature and transforms to the tetragonal structure during temperature quench. If the tetragonal structure is indeed stable at the high P–T conditions of the Earth's transition zone and lower mantle, elastic properties and their direction dependencies can be very different from those expected for a cubic structure, as shown in the case of $SrTiO_3$ perovskite [*Okai and Yoshimoto*, 1975; *Fischer et al.*, 1989]. It is also important to investigate whether a cubic-tetragonal phase transition can occur at mantle conditions. Since the dodecahedral site (Ca site) of Ca-pv provides the main repository of large cations in the deep mantle [*Kato et al.*, 1988], the distortion of this site in the tetragonal structure can influence the partitioning of trace elements, such as U, Th, and Sr. High-temperature XRD and elasticity measurements will be important to answer these remaining questions.

[21] **Acknowledgments.** This work was supported in part by NSF, the Miller intstitute (to SS), and the David and Lucile Packard foundation (to TD). We thank for discussions with L. Stixrude, C. Prewitt, B. Kiefer, and an anonymous reviewer. W. H. Choi and C.-S. Zha assisted in the XRD measurements.

References

Akber-Knutson, S., M. S. T. Bukowinski, and J. Matas, On the structure and compressibility of $CaSiO_3$ perovskite, *Geophys. Res. Lett.*, *29*, 10.1029/2001GL013523, 2002.

Desgreniers, S., SImPA - user guide, *Tech. rep.*, University of Ottawa, 1998.

Dollase, W. A., Correction of intensities for preferred orientation in powder diffractometry: Application of the March model, *J. Appl. Crystallogr.*, *19*, 267–272, 1986.

Fischer, M., B. Bonello, A. Polian, J.-M. Leger, A. Polian, and J.-M. Léger, Elasticity of $SrTiO_3$ perovskite under high pressure, in *Perovskite: A Structure of Great Interest to Gephysics and Materials Science*, edited by A. Navrotsky and D. J. Weidner, vol. 45 of *Geophysical Monograph*, pp. 125–130, American Geophysical Union, 1989.

Funamori, N., R. Jeanloz, N. Miyajima, and K. Fujino, Mineral assemblages of basalt in the lower mantle, *J. Geophys. Res.*, *105*, 26,037–26,043, 2000.

Glazer, A. M., The classification of tilted octahedra in perovskites, *Acta Crystallogr.*, *B28*, 3384–3392, 1972.

Holland, T. J. B., and S. A. T. Redfern, Unit cell refinement from powder diffraction data: the use of regression diagnostics, *Mineral. Mag.*, *61*, 65–77, 1997.

Holmes, N. C., J. A. Moriarty, G. R. Gathers, and W. J. Nellis, The equation of state of platinum to 660 GPa (6.6 Mbar), *J. Appl. Phys.*, *66*, 2962–2967, 1989.

Horiuchi, H., E. Ito, and D. J. Weidner, Perovskite-type $MgSiO_3$: single-crystal X-ray diffraction study, *Am. Mineral.*, *72*, 357–360, 1987.

Kato, T., A. E. Ringwood, and T. Irifune, Experimental-determination of element partitioning between silicate perovskites, garnets and liquids - constrains on early differentiation of the mantle, *Earth Planet. Sc. Lett.*, *89*, 123–145, 1988.

Kudoh, Y., E. Ito, and H. Takeda, Effect of pressure on the crystal structure of perovskite-type $MgSiO_3$, *Phys. Chem. Mineral.*, *14*, 350–354, 1987.

Larson, A. C., and R. B. Von Dreele, GSAS manual, *Tech. Rep. LAUR* 86-748, Los Alamos National Laboratory, 1988.

Magyari-Köpe, B., L. Vitos, G. Grimvall, B. Johansson, and J. Kollár, Low-temperature crystal structure of $CaSiO_3$ perovskite: An ab initio total energy study, *Phys. Rev. B Condens. Matter*, *65*, 193,107, 2002.

Mao, H.-K., L. C. Chen, R. J. Hemley, A. P. Jephcoat, and Y. Wu, Stability and equation of state of $CaSiO_3$-perovskite to 134 GPa, *J. Geophys. Res.*, *94*, 17,889–17,894, 1989.

Okai, B., and J. Yoshimoto, Pressure dependence of the structural phase transition temperature in $SrTiO_3$ and $KMnF_3$, *J. Phys. Soc. Jpn.*, *39*, 162–165, 1975.

Ross, N., and R. M. Hazen, Single crystal X-ray diffraction study of $MgSiO_3$ perovskite from 77 to 400 K, *Phys. Chem. Mineral.*, *16*, 415–420, 1989.

Shim, S.-H., T. S. Duffy, and G. Shen, The equation of state of $CaSiO_3$ perovskite to 108 GPa at 300 K, *Phys. Earth Planet. Inter.*, *120*, 327–338, 2000a.

Shim, S.-H., T. S. Duffy, and G. Shen, The stability and P-V-T equation of state for $CaSiO_3$ perovskite in the earth's lower mantle, *J. Geophys. Res.*, *105*, 25,955–25,968, 2000b.

Singh, A. K., The lattice strains in a specimen (cubic system) compressed nonhydrostatically in an opposed anvil device, *J. Appl. Phys.*, *73*, 4278–4286, 1993.

Sinogeikin, S. V., and J. D. Bass, Elasticity of majorite and a majorite-pyrope solid solution to high pressure: Implications for the transition zone, *Geophys. Res. Lett.*, *29*, 10.1029/2001GL013937, 2002.

Stixrude, L., R. E. Cohen, R. Yu, and H. Krakauer, Prediction of phase transition in $CaSiO_3$ perovskite and implications for lower mantle structure, *Am. Mineral.*, *81*, 1293–1296, 1996.

Tamai, H., and T. Yagi, High-pressure and high-temperature phase relations in $CaSiO_3$ and $CaMgSi_2O_6$ and elasticity of perovskite-type $CaSiO_3$, *Phys. Earth Planet. Inter.*, *54*, 370–377, 1989.

Tarrida, M., and P. Richet, Equation of state of $CaSiO_3$ perovskite to 96 GPa, *Geophys. Res. Lett.*, *16*, 1351–1354, 1989.

Wang, Z., and T. Yagi, Incorporation of ferric iron in $CaSiO_3$ perovskite at high pressure, *Mineral. Mag.*, *62*, 719–723, 1998.

Wang, Y., D. J. Weidner, and F. Guyot, Thermal equation of state of $CaSiO_3$ perovskite, *J. Geophys. Res.*, *101*, 661–672, 1996.

Wood, B. J., Phase transformations and partitioning relations in peridotite under lower mantle conditions, *Earth Planet. Sc. Lett.*, *174*, 341–354, 2000.

Woodward, P. M., Octahedral tilting in perovskites, I. geometrical consideration, *Acta Crystallogr.*, *B53*, 32–43, 1997.

Yagi, T., S. Kusanagi, Y. Tsuchida, and Y. Fukai, Isothermal compression and stability of perovskite-type $CaSiO_3$, *P. Jpn. Acad. B-Phys.*, *65*, 129–132, 1989.

T. S. Duffy, Department of Geosciences, Princeton University, Princeton, NJ 08544, USA. (duffy@princeton.edu)

R. Jeanloz and S.-H. Shim, Department of Earth and Planetary Science, University of California, Berkeley, CA 94720, USA. (jeanloz@uclink.berkeley.edu; sangshim@uclink.berkeley.edu)